AJNR Am J Neuroradiol 22:1711–1718, October 2001

Reliability of Functional MR Imaging with Word-Generation Tasks for Mapping Broca's Area

John H. Brannen, Behnam Badie, Chad H. Moritz, Michelle Quigley, M. Elizabeth Meyerand, and Victor M. Haughton

BACKGROUND AND PURPOSE: **Functional MR (fMR) imaging of word generation has been used to map Broca's area in some patients selected for craniotomy. The purpose of this study was to measure the reliability, precision, and accuracy of word-generation tasks to identify Broca's area.**

METHODS: **The Brodmann areas activated during performance of word-generation tasks were tabulated in 34 consecutive patients referred for fMR imaging mapping of language areas. In patients performing two iterations of the letter word-generation tasks, test-retest reliability was quantified by using the concurrence ratio (CR), or the number of voxels activated by each iteration in proportion to the average number of voxels activated from both iterations of the task. Among patients who also underwent category or antonym word generation or both, the similarity of the activation from each task was assessed with the CR. In patients who underwent electrocortical stimulation (ECS) mapping of speech function during craniotomy while awake, the sites with speech function were compared with the locations of activation found during fMR imaging of word generation.**

RESULTS: **In 31 of 34 patients, activation was identified in the inferior frontal gyri or middle frontal gyri or both in Brodmann areas 9, 44, 45, or 46, unilaterally or bilaterally, with one or more of the tasks. Activation was noted in the same gyri when the patient performed a second iteration of the letter word-generation task or second task. The CR for pixel precision in a single section averaged 49%. In patients who underwent craniotomy while awake, speech areas located with ECS coincided with areas of the brain activated during a word-generation task.**

CONCLUSION: **fMR imaging with word-generation tasks produces technically satisfactory maps of Broca's area, which localize the area accurately and reliably.**

Functional MR (fMR) imaging is used to map eloquent brain regions before craniotomy because it depicts these regions more reliably and accurately than do anatomic landmarks visualized on MR images (1, 2). According to one report, fMR imaging shows a ''high degree of promise for language location for presurgical planning'' (3). In previous reports, many different language tasks have been used, and activation in multiple lobes of the brain has been identified. For the identification of Broca's area in the frontal lobe, language tasks, such as covert word generation from letters, categories, or antonyms, have seemed to be effective. To our knowledge, the reliability and precision of these tasks in a large series of patients have not been reported. The purpose of this study was to determine the reliability, test-retest precision, and accuracy of the standard word-generation paradigms for fMR imaging. For precision, we used a concurrence ratio (CR) between the first and second iterations of the task; for accuracy, we compared the results of functional imaging with those of intraoperative mapping.

Received December 6, 2000; accepted after revision May 13, 2001.

From the Departments of Radiology (J.H.B., C.H.M., V.M.H.), Neurosurgery (B.B.), and Medical Physics (M.Q., M.E.M.), University of Wisconsin, Madison.

Address reprint requests to Victor Haughton, MD, Department of Radiology, Clinical Sciences Center, Module E3, 600 Highland Avenue, Madison, WI 53792.

Methods

Patients

We retrospectively reviewed 34 patients with cerebral lesions who were referred for fMR imaging language mapping between January 1999 and July 2000. Each patient had per-

formed one or more covert word-generation tasks. For each patient, we tabulated the location of activation from a word-generation task. For those who performed more than one language task, we also measured the agreement between iterations of the task. Finally, we also studied the agreement with results of electrocortical stimulation (ECS) mapping from subsequent craniotomy, obtained while the patient was awake, if available.

Analysis of Activation

In the tabulation of activation from word-generation tasks, five contiguous coronal sections encompassing the middle and inferior frontal gyri were examined. A threshold was chosen for each study, which provided 10–14 activated voxels within the selected sections. In all patients but one, the threshold chosen had an uncorrected *P* value of .001. For patient 28, the threshold chosen had a *P* value of .005. In patients 3, 5, and 19, in whom no activation was identified at a threshold of $P = .001$, multiple thresholds were used without the identification of activation. In each case, we assigned the location of activation to Brodmann areas 9, 44, 45, and/or 46, on the basis of standard parcellation methods and standard texts (4). Brodmann area 9 was defined as the middle frontal gyrus superior to the pars opercularis of the inferior frontal gyrus; Brodmann area 44, as the pars opercularis of the inferior frontal gyrus; Brodmann area 45, as the pars triangularis of the inferior frontal gyrus; and Brodmann area 46, as the middle frontal gyrus superior to and the inferior frontal sulcus anterior to the pars triangularis. Activation encompassing the inferior frontal sulcus was assigned to the Brodmann area with which it was most closely associated. If the activation was equally distributed between the middle and inferior frontal gyri, the activation was assigned to both bordering Brodmann areas. If the activation was outside of the Brodmann areas 9, 44, 45 and 46, it was not tabulated.

Test-retest precision was calculated for the patients who performed more than one iteration of the letter word-generation (LWG) task. For this analysis, we set the threshold for the five contiguous coronal sections encompassing the inferior frontal gyrus at $P = .001$. The number of voxels activated both in the first and second iterations of the task was determined, and these voxels were displayed as the intersect map. The number of pixels in the intersect map was divided by the average number of pixels on each map. This product was defined as the CR (5). The CR was determined for each case and averaged for all cases with two iterations of the task. We also determined the CR for the single section in each case with the greatest amount of activation.

The similarity of activation patterns between different versions of the word-generation task was analyzed in all patients who underwent category word-generation (CWG) and/or antonym word-generation (AWG) tasks in addition to LWG tasks. We set a threshold of $P = .001$ for the functional maps for each task. The intersect map and CR were determined as just described.

Operative records were reviewed to identify patients who also underwent ECS mapping of speech function assessed during craniotomy while awake. ECS had been performed as described by Berger and Ojemann (6). Briefly, after craniotomy and opening of the dura, the cortex was stimulated with a bipolar probe with a 3–5-s train of square-wave pulses (500 ms/phase at 50 Hz). The intensity of the stimulus gradually was increased by increments of 2 mA (to 14.5 mA) until speech arrest or after-discharges occurred. Both receptive and expressive language functions were assessed by evaluating repetition, command following, and confrontation naming. If cortical stimulation led to speech arrest, then the region of the brain was marked as a speech region. The neurosurgeon determined the location of this region at the time of ECS without reference to the fMR images. After mapping, the surface of the brain was photographed to record the positions of the speech areas. The same parcellation techniques used to localize the fMR imaging activation also were used to describe the sites of function identified intraoperatively. We determined the agreement between the ECS and fMR imaging localizations by comparing the Brodmann areas assigned for each method.

Each patient underwent fMR imaging performed with a 1.5-T commercial imager equipped with high-speed gradients, with techniques previously reported (7). Preliminary anatomic images were obtained with multisection, spin-echo sequences. Single-shot echo-planar images were acquired in the coronal plane every other second for 228 s. Technical parameters for these images included the acquisition of 114 images, 20 section locations, a 64×64 matrix, a flip angle of 85°, 2/40 (TR/TE), a field of view of 24 cm, a section thickness of 6 mm with a gap of 1 mm, and a bandwidth ± 62.5 kHz.

For each of the three word-generation tasks, patients were asked to lie motionless in the imager. Each task consisted of five 20-s blocks of task performance interspersed with 20-s rest periods during which patients were instructed to refrain from generating words and from cognitive effort as much as possible. During the task period, the patients were instructed to covertly generate as many words as possible when cued. In the LWG task, the patient was verbally cued with a letter from the alphabet at the beginning of each task period and asked to think of as many words as possible that begin with that letter. The patients were given a different letter for each of the five task periods. The auditory cues were presented though earphones by means of an intercom. In the CWG task, a different category was verbally given to the patient at the beginning of each task period, and the patient was instructed to think of words that belonged to that category for 20 s. Categories such as ''animals'' and ''things found in a house'' were used. In the AWG task, the patient was shown a series of 10 words (presentation rate, one word every 2 s) in each 20-s task cycle and instructed to think of antonyms for each word. The visual cues were projected onto a screen that the patient viewed through prism mirrors.

For postprocessing of the fMR images, echo-planar raw data were low-pass filtered in the spatial frequency domain by using a Hamming filter (8). The data were then reconstructed into individual section-location time courses. These reconstructed time-course files then were checked for patient head motion and realigned by using a 3D spatial-registration algorithm (9). A signal-to-noise threshold was applied to mask background voxels from further analysis. The time course plots from each unmasked echo-planar image voxel were compared with reference functions by using a generalized least-squares-fitting algorithm, fitting the observed data on a voxel-by-voxel basis to sets of user-defined functions. The fitted functions included a constant (baseline signal level), a ramp (to allow for possible linear signal drift), a temporal smoothing filter (to compensate for the differences in image-acquisition times within each 2-s TR), and a smoothed boxcar reference function that modeled the presumed stimulus responses.

Results

Findings were reviewed for 34 patients who were examined between February 1999 and July 2000. For 31 of the 34 patients, we obtained activation maps of good technical quality with one or more word-generation tasks. In two of the patients who lacked good-quality maps, motion had corrupted the data; in the third, no motion was evident, and poor task compliance was assumed to be responsible for the technical failure.

In the 31 patients, 18 had activation of the left hemisphere exclusively, 10 had activation bilaterally, and three had activation of the right hemisphere exclusively. Of the 18 patients with left-hemisphere activation, activation was in Brodmann area 44 in 66% of cases, Brodmann area 46 in 61%, Brodmann area

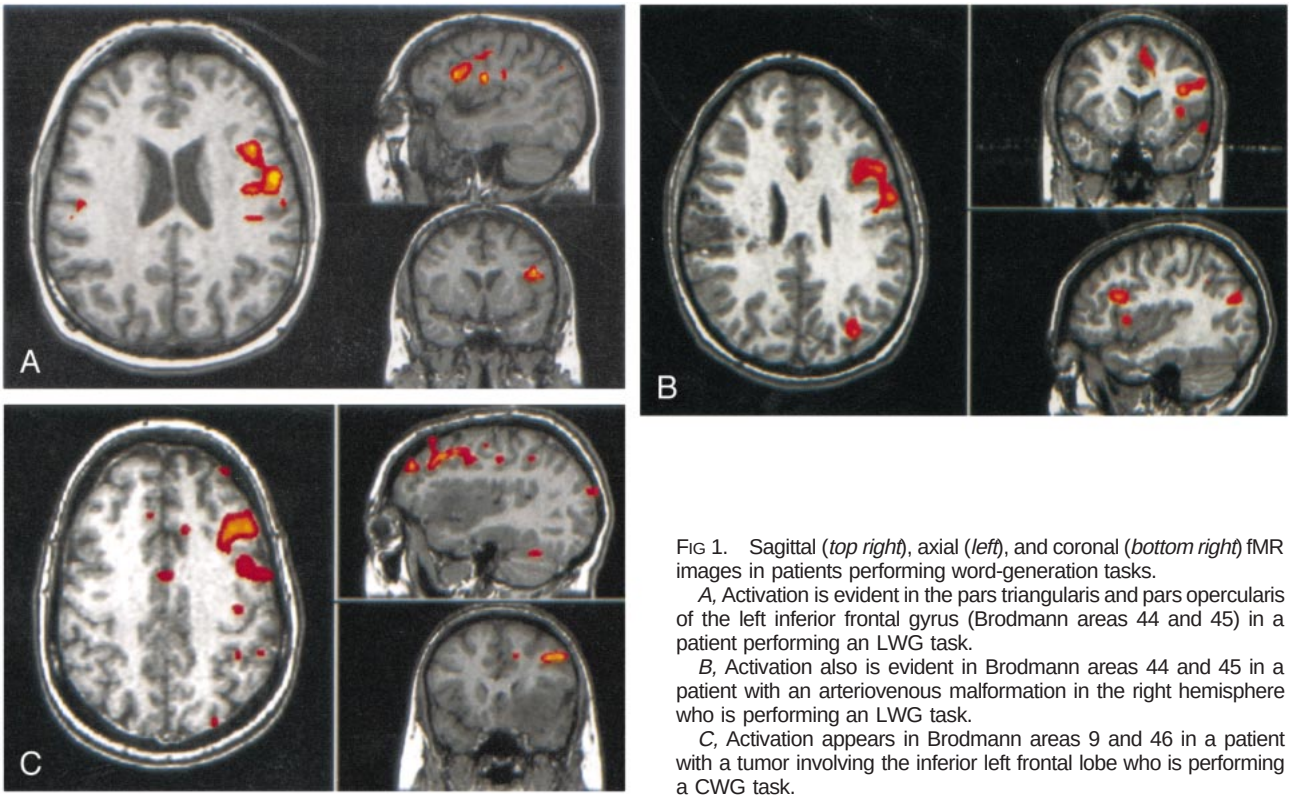

FIG 1. Sagittal (*top right*), axial (*left*), and coronal (*bottom right*) fMR images in patients performing word-generation tasks.

A, Activation is evident in the pars triangularis and pars opercularis of the left inferior frontal gyrus (Brodmann areas 44 and 45) in a patient performing an LWG task.

B, Activation also is evident in Brodmann areas 44 and 45 in a patient with an arteriovenous malformation in the right hemisphere who is performing an LWG task.

C, Activation appears in Brodmann areas 9 and 46 in a patient with a tumor involving the inferior left frontal lobe who is performing a CWG task.

9 in 44%, or Brodmann area 45 in 39% (Fig 1). In the 10 patients with activation of both frontal lobes, the activation was in the left Brodmann area 44 in 60% of patients, left Brodmann area 46 in 50%, left Brodmann area 45 in 30%, or left Brodmann area 9 in 10%. These same 10 patients also had activation in right Brodmann area 44 (20% of patients), right Brodmann area 45 (20%), right Brodmann area 46 (70%), or right Brodmann area 9 (40%). In the three patients with right hemispheric activation alone, the activation was in Brodmann area 44 (67% of patients), Brodmann area 45 (67%), Brodmann area 9 (67%), or Brodmann area 46 (33%) (Table 1) (Fig 2).

Twelve patients underwent two iterations of the LWG task. The activation from the first and second iteration of the task was located in the same Brodmann areas (Fig 3). The maps for the first and second iterations of the task were similar (Fig 4). The CR (ie, the number of voxels shared by the five sections in the two activation maps divided by the average of the total number of active voxels in both maps) ranged from 17% to 57%. The mean CR for the group was 37% (Table 2). In the patients with the lowest CRs (17% and 22%), one iteration of the task appeared to have a high noise level or poor task performance. The CRs of matched individual sections ranged up to 74%. The mean CR for all patients for a single section was 49% (Table 3).

In nine patients who underwent CWG and/or AWG in addition to LWG, activation was in the same Brodmann locations for each task (Figs 5 and 6). Four patients underwent both LWG and AWG tasks; three patients underwent both CWG and LWG tasks; and two patients underwent LWG, AWG, and CWG tasks. Six comparisons were made between LWG and AWG tasks, four were made between CWG and LWG tasks, and two were made between AWG and CWG tasks. The CRs for the five-section locations for the AWG-to-CWG comparisons ranged from 39% to 44% with a mean of 42%. The CRs for the five sections for CWG-to-LWG comparisons ranged from 9% to 60%, with a mean of 42%. The CRs for the five sections for the LWG-to-CWG comparisons ranged from 33% to 44% with a mean of 37%. The mean CR for all of the five-section location comparisons was 39% (Table 4). For a single section, the CRs were as high as 65%. The mean CR for the single sections was 51% (Table 5). In the patient with the lowest CR (single section CR, 21%), both the LWG and CWG tasks appeared to have high noise level or poor task performance.

Seven patients underwent both ECS of speech function and mapping of language with fMR imaging (Table 6). With ECS, speech function was found in Brodmann area 44 (71% of patients) and Brodmann area 45 (57% of patients). In six of the seven patients, the speech-area activation located with ECS coincided with areas of brain activated during their word-generation task (Fig 7). In the remaining patient, activation from the word-generation task could be placed in the same gyrus as that located with ECS for speech function, but the tumor obscured cerebral landmarks, making assignment to Brodmann area 44 or 45 uncertain. In five of the seven patients, mapping with fMR imaging revealed additional areas of lan-

TABLE 1: Location of activation, threshold for fMR images, word-generation paradigm, and clinical diagnosis in the 31 patients with activation

Patient No.	Area of Activation		Paradigm	Disease
	Left	Right		
1	44, 46	44, 46	LWG	L temporoparietal tumor
2	44, 46	44, 45	LWG	L frontoparietal AVM
3	None	None	LWG	L middle cerebral artery malformation
4	44, 46	None	LWG	L frontal glioma
5	None	None	LWG	R frontal tumor, partial motor seizures
6	44	None	LWG	L frontal anaplastic astrocytoma
7	9, 45, 46	None	LWG	L medial frontal, superior-middle temporal diffuse oligodendroglioma
8	9, 44, 46	None	LWG	L middle cerebral AVM
9	46	None	LWG	L temporal oligodendroglioma
10	9, 44, 45	None	LWG	L parietal AVM
11	44, 45	None	LWG	R parasylvian AVM
12	9, 44	None	LWG	L parietal cavernous angioma
13	44, 45	None	LWG	L basal ganglia tumor
14	44, 45	46	LWG	R posterior temporal glioblastoma multiforme
15	44	45, 46	LWG	L posterior parietal AVM
16	9, 46	None	LWG	L temporooccipital AVM
17	None	9, 44	LWG	L frontal tumor
18	9, 46	None	LWG	L frontal glioma
19	None	None	AWG	L basal ganglia tumor
20	None	9, 44, 45	LWG	L posterior frontal tumor
21	46	9, 46	LWG	R frontal parietal tumor
22	44, 45, 46	46, 9	LWG	L frontal fibrillary astrocytoma
23	9	9	LWG	L frontal glioma
24	46	None	LWG	L frontal glioma
25	9, 44, 46	None	LWG	R parasagittal meningioma
26	44, 45, 46	None	LWG	R frontal glioma
27	44, 45	None	LWG	R temporal AVM
28	45, 46	9	LWG	L frontal tumor
29	44, 45	None	LWG	R frontal parietal AVM
30	None	46	LWG	L frontal tumor
31	9, 46	None	AWG	R parietal tumor
32	44	46	LWG	L frontal lobe, low-grade glioma
33	None	45, 46	LWG	L frontal temporal glioma
34	44, 46	None	LWG	L frontal tumor

Note.—AVM indicates arteriovenous malformation; L, left; R, right.

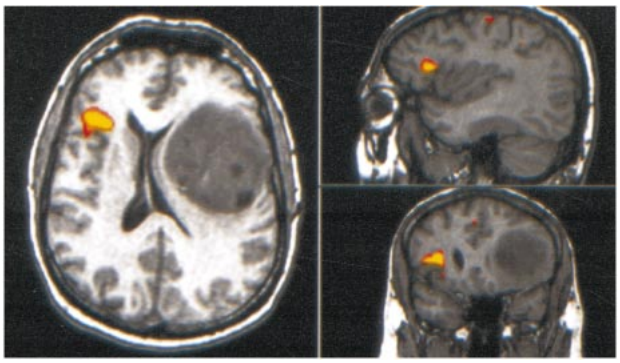

FIG 2. Sagittal (*top right*), axial (*left*), and coronal (*bottom right*) fMR images in a patient with a large left frontal tumor who is performing an LWG task. Activation is identified primarily in the right inferior frontal gyrus (Brodmann area 45).

guage activation not identified by the ECS. These were located in Brodmann area 9 (43% of patients) and Brodmann area 46 (43% of patients). These areas had not been studied at ECS because of the limited surgical exposure.

Discussion

In this study, word-generation tasks activated Brodmann areas 44, 46, or both in most patients in the series. Brodmann areas 9 and 45 also were activated frequently. These areas were activated whether language dominance was left, right, or mixed. Most areas activated in one iteration or one version of a task were activated if a second iteration or version was performed. The language activation was accurate rate compared with intraoperative mapping in the seven patients who underwent both fMR imaging and ECS.

The accuracy of fMR imaging in the identification of Broca's area in this study substantially agrees with

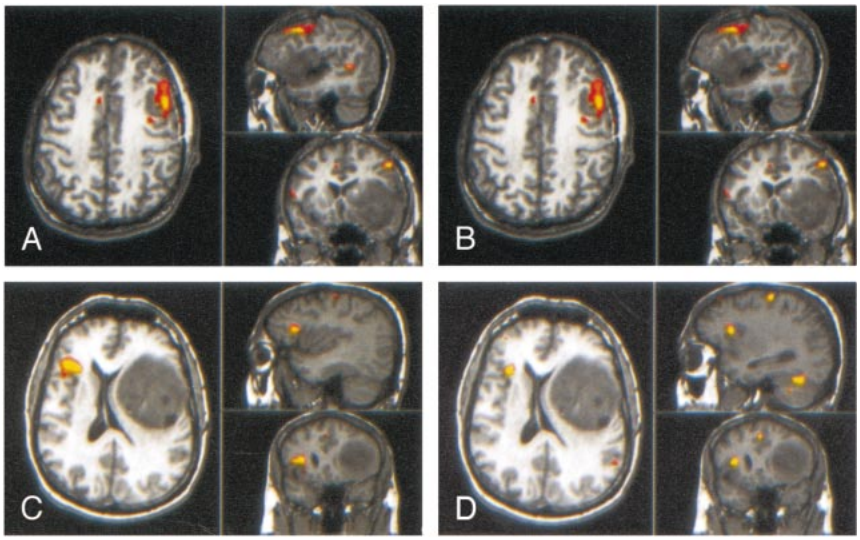

FIG 3. Sagittal (*top right*), axial (*left*), and coronal (*bottom right*) activation images in two iterations of an LWG task.

A and *B,* Patient with a left frontal tumor. Activation occurs in the same gyri between iterations, although with slightly different patterns.

C and *D,* Patient with a left frontal tumor and right hemispheric activation.

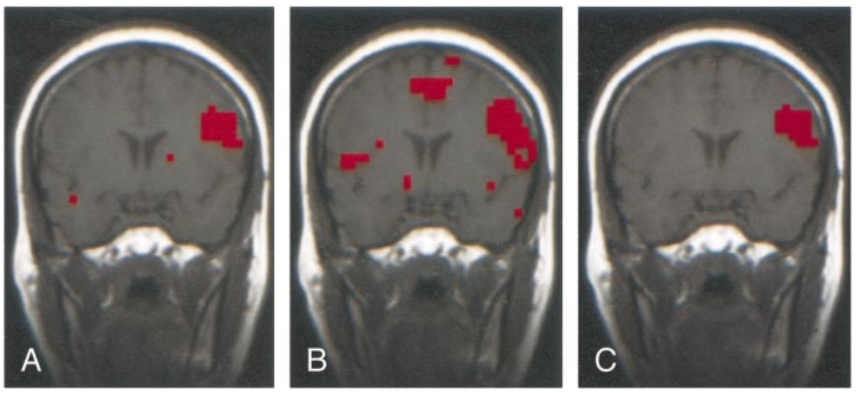

FIG 4. Coronal fMR imaging images of two iterations of an LWG task in a patient with a left middle cerebral arteriovenous malformation.

A, Activation in the first iteration.

B, Activation in the second iteration, showing similar activation compared with *A.*

C, Intersect map shows the voxels activated in the two iterations. The proportion of voxels in the intersect map compared with the average number of voxels in *A* and *B* (the CR) is 45%.

TABLE 2: CRs for five-section comparisons in patients performing two iterations of an LWG task

Patient No.	CR (%)
6	37
8	28
9	56
13	34
14	51
15	57
17	25
18	45
20	33
21	17
22	42
23	22
Mean	37

TABLE 3: CRs for single-section comparisons in patients performing two iterations of an LWG task

Patient No.	CR (%)
6	45
8	45
9	63
13	47
14	59
15	74
17	38
18	60
20	41
21	20
22	50
23	48
Mean	49

that of previous reports. FitzGerald et al (3) reported that in 85% of comparisons in 11 patients performing visual verb generation, performing auditory verb generation, listening to narrated text, listening to words, or reading words, activation was found to register to within 1 cm of the site of ECS language function. In their study, the accuracy for Broca's area alone was not tabulated separately from the accuracy for other regions. In our study, the Brodmann area in which activation was identified corresponded in each of seven cases to the area in which language function was found with ECS.

We used methods that have been used to test the precision and accuracy of fMR imaging. To compare

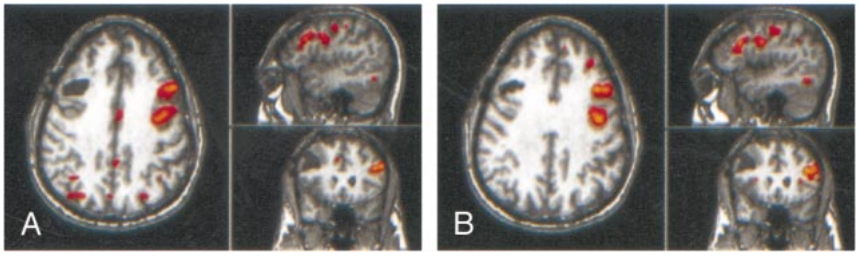

FIG 5. Sagittal (*top right*), axial (*left*), and coronal (*bottom right*) projections in a patient with a right frontal tumor.
A, Activation from a CWG task.
B, Activation from an LWG task.

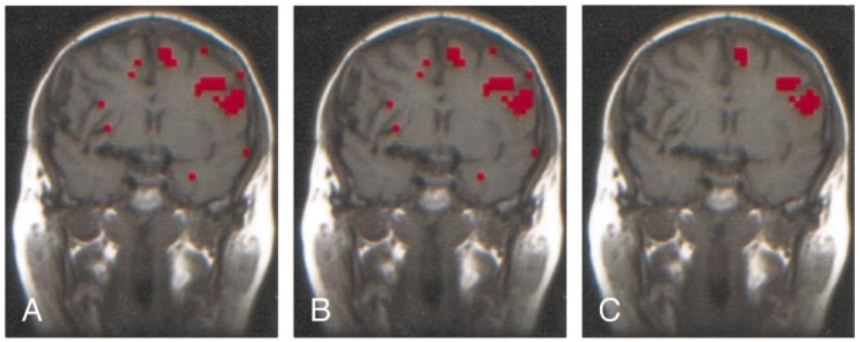

FIG 6. Coronal images in a patient with a right frontoparietal arteriovenous malformation.
A, Activation from an AWG task
B, Activation from a CWG task. The activation patterns from the two variations of the word-generation task are similar.
C, Intersect map shows the voxels activated by both versions of the task. The CR was 52%.

TABLE 4: CRs for five-section comparisons in patients performing two or more versions of the language task

Task Comparison and Patient No.	CR (%)
LWG vs AWG	
24	44
29	38
32	34
30	33
34	34
33	36
Mean	37
CWG vs LWG	
24	55
26	60
33	42
28	9
Mean	42
AWG vs CWG	
24	44
33	39
Mean	42
All, mean	39

TABLE 5: CRs for single-section comparisons in patients performing two iterations of the language task

Task Comparison and Patient No.	CR (%)
LWG vs AWG	
24	55
29	52
32	55
30	48
34	56
33	41
Mean	51
CWG vs LWG	
24	63
26	65
33	46
28	21
Mean	49
AWG vs CWG	
24	54
33	53
Mean	54
All, mean	51

test-retest precision, we used the intersect map and the CR developed by Quigley et al (5). Both single- and multiple-section comparisons were made. In the comparison of the fMR imaging activation with intraoperative localization of function, we elected not to register planar fMR images with photos of the brain surface or to use the navigational workstation, as others have (3, 10, 11). Photos of the brain surface with embedded functional information cannot be precisely coregistered with the planar images at fMR imaging. The surgeon did not have functional data embedded in the image files in the workstation for this study. Therefore, we elected to describe the location of activation in terms of Brodmann areas. In most cases, the Brodmann area was readily determined by identifying the inferior frontal sulcus and the ascending rami within the inferior frontal gyrus. In cases in which a cluster of activation appeared to be centered on the inferior frontal sulcus, the assignment to one or two Brodmann areas was more equivocal. Therefore, the number of times that one of the

TABLE 6: Brodmann area of speech function in patients undergoing both ECS and fMR imaging

Patient No.	Brodmann Area at ECS	Brodmann Area at fMR Imaging
1	44	44
6	44	44
13	44,45	44, 45
18	44	44, 46, 9
22	45	45, 46, 44
23	44, 45	Inferior frontal gyrus, 9
24	45	45, 9, 46

Brodmann areas was activated may have been slightly overestimated.

Our gross anatomic comparison has advantages compared with graphic techniques. It is less affected by geometric distortion, and it overcomes the difficulty in determining criteria for perfect coregistration. We controlled for reader bias by having different investigators localize the eloquent cortex with fMR imaging and ECS. The likelihood that the surgeon was biased by the fMR images in identifying the language area seems small, because exact speech mapping is crucial for optimizing surgical results. The volume of a region in which function is identified with ECS is estimated to be on the order of 1 cm (3).

We found that the single-section test-retest precision for LWG was 49% and precision values were similar if two versions of the word-generation task were performed. For motor, sensory, and visual tasks, precision measurements of 57%, 57%, and 74%, respectively, have been reported with similar techniques (12, 13). Some of the differences between the precision for language tasks versus visual tasks may be explained by variation in fMR imaging and image-processing techniques. However, the fMR imaging techniques that we used did not differ in important ways, we believe, from those of other studies. As in other studies of fMR imaging precision in patients, we used a threshold that produced equivalent amounts of activation in each patient, rather than a fixed threshold, which would have produced excessive interindividual variations in the amount of activation. Differences in the patient's performance in the first and second iterations of the word-generation task likely explain the lower test-retest precision scores.

We did not attempt to identify areas of language activation outside the frontal lobe, to use a battery of language tasks, or to determine hemispheric dominance for language, which was the focus of other reports (3, 14, 15). Activation has been reported in Broca's area, the left middle temporal gyrus, the left superior temporal gyrus, and Wernicke's area in patients performing various language tasks (3). The focus of this study was the word-generation task and Broca's area.

The fraction of patients with mixed and right hemispheric activation was larger than the proportion of right hemispheric dominance in the normal population. We found that 10% of the patients had right hemispheric activation, and 32% had bilateral activation. Reasons for such a difference have been discussed previously (3). The difference between our patient group and the normal population probably is attributable to bias in the selection of patients for clinical referral, brain plasticity induced by nearby cerebral lesions, or both.

Conclusion

The reliability, precision, and accuracy of functional MR imaging with word generation differs only slightly from reported measures for fMR imaging mapping of motor and visual cortices. Localization of Broca's area by using fMR imaging with word-generation tasks has been robustly demonstrated in a diverse group of preoperative patients.

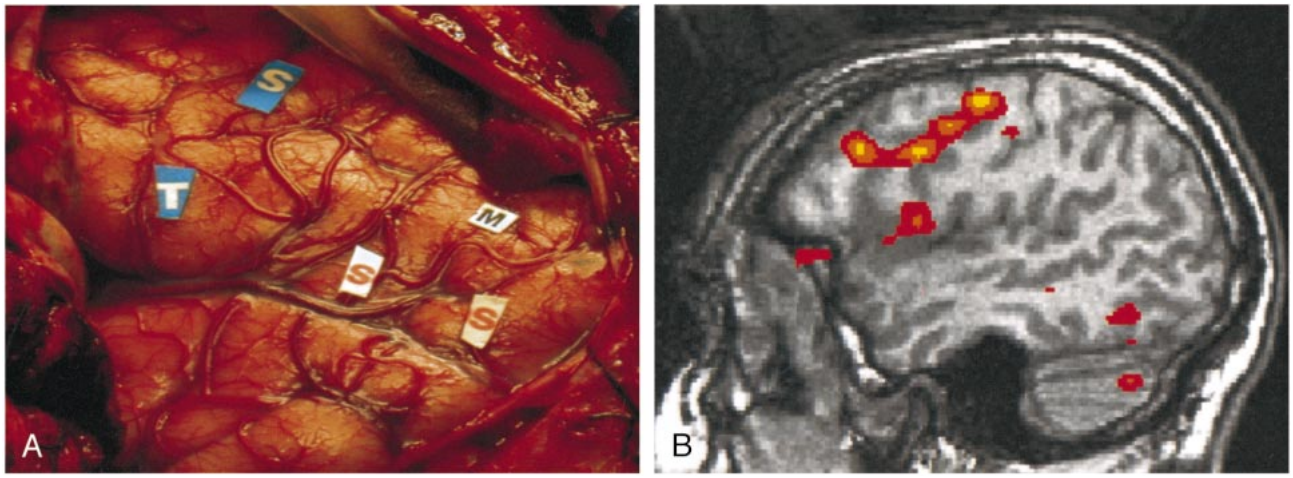

FIG 7. Comparison of intraoperative localization of speech function (ECS) and activation from the word-generation task (fMR imaging) in a patient with a left frontal-lobe glioma. Both activation and intraoperative localization of the speech mapping were classified as belonging to Brodmann areas 44 and 45. *M* indicates motor cortex; *S,* speech areas; *T,* tumor.

References

1. Yetkin FZ, Papke RA, Daniels DL, Mueller WM, Haughton VM. **Location of the sensorimotor cortex: functional and conventional MR compared.** *AJNR Am J Neuroradiol* 1995;16:2109–2113
2. Sobel DF, Gallen CC, Schwartz BJ, et al. **Locating the central sulcus: comparison of MR anatomic and magnetoencephalographic methods.** *AJNR Am J Neuroradiol* 1993;4:915–925
3. FitzGerald DB, Cosgrove GR, Ronner S, et al. **Location of language in the cortex: a comparison between functional MR imaging and electrocortical stimulation.** *AJNR Am J Neuroradiol* 1997;19: 1529–1539
4. Talairach J, Tournoux P. **Co-planar stereotaxic atlas of the human brain.** In: *3-Dimensional Proportional System: An Approach to Cerebral Imaging.* New York, NY: Thieme Medical Publishers; 1988
5. Quigley M, Cordes D, Wendt G, et al. **Effect of focal and non-focal cerebral lesions on functional connectivity studied with MR.** *AJNR Am J Neuroradiol* 2001;(in press)
6. Berger MS, Ojemann GA. **Techniques of functional localization during removal of tumors involving the cerebral hemispheres.** In: Loftus CM, Traynelis VC, eds. *Intraoperative Monitoring Techniques in Neurosurgery*. New York, NY: McGraw-Hill; 1994;113–127
7. Lowe MJ, Sorenson JA. **Spatially filtering functional magnetic resonance imaging data.** *Magn Reson Med* 1997;37:723–739
8. Lowe MJ, Russell DP. **Treatment of baseline drifts in fMRI time series analysis.** *J Comput Assist Tomogr* 1999;23:463–473
9. Cox. RW **AFNI: software for analysis and visualization of functional magnetic resonance neuroimages.** *Comput Biomed Res* 1996; 29:162–173
10. Jack C Jr, Thompson RM, Butts RK, et al. **Sensory motor cortex: correlation of presurgical mapping with functional MR imaging and invasive cortical mapping.** *Radiology* 1994;190:85–92
11. Holodny AI, Schulder M, Liu WC, Wolki J, Maldjian JA, Kalnin AJ. **The effect of brain tumors on BOLD functional MR imaging activation in the adjacent motor cortex: implications for image-guided neurosurgery.** *AJNR Am J Neuroradiol* 2000;21:1415–1422
12. Yetkin FZ, McAuliffe TL, Cox R, Haughton VM. **Test-retest precision of functional MR in sensory and motor task activation.** *AJNR Am J Neuroradiol* 1996;17:579–584
13. Rombouts SA, Barkhof F, Hoogenraad FG, Sprenger M, Scheltens P. **Within-subject reproducibility of visual activation patterns with functional magnetic resonance imaging using multislice echo planar imaging.** *Magn Reson Imaging* 1998;16:105–113
14. Benson RR, FitzGerald DB, LeSeur LL, et al. **Language dominance determined by whole brain functional MRI in patients with brain lesions.** *Neurology* 1999;52:798–809
15. Binder JR, Swanson SJ, Hammeke TA, et al. **Determination of language dominance using functional MRI: a comparison with the Wada test.** *Neurology* 1996;46:978–84